

Modified parameter-sets of M3Y-type semi-realistic nucleon-nucleon interaction for nuclear structure studies

H. Nakada*

*Department of Physics, Graduate School of Science, Chiba University
Yayoi-cho 1-33, Inage, Chiba 263-8522, Japan*

(Dated: October 29, 2018)

Abstract

New parameter-sets of the M3Y-type semi-realistic nucleon-nucleon interaction are obtained, by taking into account the whole contribution of the interaction to the pairing. The interactions are applicable to nuclear structure studies via mean-field calculations and their extensions. Implementing self-consistent mean-field calculations for the spherical nuclei, we confirm that the results do not change significantly from the previous ones, in which the parameters were determined by partly discarding influence of the density-dependent repulsion on the pairing.

PACS numbers: 21.30.Fe, 21.60.Jz, 21.10.Dr, 21.65.-f

arXiv:0912.0314v2 [nucl-th] 12 Jan 2010

* E-mail: nakada@faculty.chiba-u.jp

I. INTRODUCTION

Mean-field (MF) theories provide us with a basic tool to study nuclear structure from nucleonic degrees of freedom. However, it is yet difficult to reproduce structure of medium- to heavy-mass nuclei with the bare nucleon-nucleon (NN) interaction to good accuracy, and most of the MF calculations have been performed with phenomenologically determined effective interactions (or energy density functionals).

The Michigan 3-range Yukawa (M3Y) interaction [1] was obtained by fitting the Yukawa functions to Brueckner's G -matrix. As the crucial role of the chiral symmetry breaking has been recognized, it is desirable to take into account the pionic effects in the NN interaction. The M3Y interaction contains the central part of the one-pion exchange potential (OPEP) and the tensor part that is corrected due to the medium effects as well as to the ρ -meson exchange. The author has developed *semi-realistic* effective NN interactions [2, 3], by modifying the M3Y interaction so as to reproduce the saturation properties and the ℓs splitting while keeping the central part of the OPEP. The tensor channels have been pointed out to be significant in the Z - or N -dependence of the shell structure [4]. We have obtained parameter-sets in which the tensor channels are maintained (*e.g.* the set M3Y-P5), and one in which the tensor channels are dropped (M3Y-P4) [3]. By implementing MF calculations, it has been shown that semi-realistic interactions could give different shell structure from the widely used Skyrme and Gogny interactions, and that of the semi-realistic interaction including the tensor channels is often favorable if compared to the experimental data. Significance of the tensor channels in the magnetic excitations has also been confirmed [5] via calculations in the random-phase approximation.

The parameter-sets developed in Ref. [3] were obtained by fitting them to pairing properties, as well as to data of doubly magic nuclei. However, in the calculations of finite nuclei in Ref. [3], influence of the density-dependent contact force on the pairing was not fully taken into account. Because we find that this influence is not negligibly small, we propose modified parameter-sets in this report, which will be useful in future studies of nuclear structure. The new parameter-sets are refitted to the same quantities as the old ones, as will be described in the subsequent section.

II. M3Y-TYPE INTERACTION

We consider the effective NN interaction that has the following form,

$$\begin{aligned}
 v_{ij} &= v_{ij}^{(C)} + v_{ij}^{(LS)} + v_{ij}^{(TN)} + v_{ij}^{(DD)} ; \\
 v_{ij}^{(C)} &= \sum_n (t_n^{(SE)} P_{SE} + t_n^{(TE)} P_{TE} + t_n^{(SO)} P_{SO} + t_n^{(TO)} P_{TO}) f_n^{(C)}(r_{ij}) , \\
 v_{ij}^{(DD)} &= (t_\rho^{(SE)} P_{SE} \cdot [\rho(\mathbf{r}_i)]^{\alpha^{(SE)}} + t_\rho^{(TE)} P_{TE} \cdot [\rho(\mathbf{r}_i)]^{\alpha^{(TE)}}) \delta(\mathbf{r}_{ij}) ,
 \end{aligned} \tag{1}$$

TABLE I. Parameters of M3Y-type interactions.

parameters		M3Y-P4	M3Y-P4'	M3Y-P5	M3Y-P5'
$1/\mu_1^{(C)}$	(fm)	0.25	0.25	0.25	0.25
$t_1^{(SE)}$	(MeV)	8027.	8027.	8027.	8027.
$t_1^{(TE)}$	(MeV)	5503.	5671.	5576.	5576.
$t_1^{(SO)}$	(MeV)	-12000.	-12500.	-1418.	-1418.
$t_1^{(TO)}$	(MeV)	3700.	4200.	11345.	11345.
$1/\mu_2^{(C)}$	(fm)	0.40	0.40	0.40	0.40
$t_2^{(SE)}$	(MeV)	-2637.	-2765.	-2650.	-2760.
$t_2^{(TE)}$	(MeV)	-4183.	-4118.	-4170.	-4029.
$t_2^{(SO)}$	(MeV)	4500.	3000.	2880.	1700.
$t_2^{(TO)}$	(MeV)	-1000.	-800.	-1780.	-1715.
$\alpha^{(SE)}$		1	1	1	1
$t_\rho^{(SE)}$	(MeV·fm ³)	248.	180.	126.	178.
$\alpha^{(TE)}$		1/3	1/3	1/3	1/3
$t_\rho^{(TE)}$	(MeV·fm)	1142.	1155.	1147.	1128.

where $\mathbf{r}_{ij} = \mathbf{r}_i - \mathbf{r}_j$, $r_{ij} = |\mathbf{r}_{ij}|$ with i and j representing the indices of nucleons, and $\rho(\mathbf{r})$ denotes the nucleon density. P_{SE} , P_{TE} , P_{SO} and P_{TO} denote the projection operators on the singlet-even (SE), triplet-even (TE), singlet-odd (SO) and triplet-odd (TO) two-particle states. The density-dependent contact force $v_{ij}^{(DD)}$ has been added to reproduce the saturation [2]. The Yukawa function $f_n^{(X)}(r) = e^{-\mu_n^{(X)}r}/\mu_n^{(X)}r$ is assumed for $X = C$, LS and TN. The modified parameter-sets M3Y-P4' and P5' are presented in Table I, in comparison with the previous sets M3Y-P4 and P5. The non-central channels $v_{ij}^{(LS)}$ and $v_{ij}^{(TN)}$ are not changed; $v_{ij}^{(LS)}$ and $v_{ij}^{(TN)}$ of M3Y-P4' (M3Y-P5') are identical to those of M3Y-P4 (M3Y-P5) [3]. The M3Y-P5' interaction has $v_{ij}^{(TN)}$ determined from the G -matrix [6], while $v_{ij}^{(TN)} = 0$ is assumed in M3Y-P4'. Not displayed in Table I, the longest range ($n = 3$) part of $v_{ij}^{(C)}$ is kept to be $v_{OPEP}^{(C)}$ (the central channels of the OPEP). The other strength parameters are fitted to the measured binding energies of ¹⁶O and ²⁰⁸Pb and to the even-odd mass differences of the Sn isotopes, in the Hartree-Fock (HF) or the Hartree-Fock-Bogolyubov (HFB) approximation. Compared to the old sets M3Y-P4 and P5, in M3Y-P4' and P5' the SE channel is more attractive below the saturation density, and its influence on the saturation and the symmetry energies is compensated by the other central channels.

TABLE II. Nuclear matter properties at the saturation point.

		D1S	D1M	M3Y-P4'	M3Y-P5'
k_{F0}	(fm ⁻¹)	1.342	1.346	1.340	1.340
\mathcal{E}_0	(MeV)	-16.01	-16.02	-16.05	-16.14
\mathcal{K}	(MeV)	202.9	225.0	230.4	239.1
M_0^*/M		0.697	0.746	0.653	0.637
a_t	(MeV)	31.12	28.55	28.49	28.42
a_s	(MeV)	26.18	16.56	23.35	23.70
a_{st}	(MeV)	29.13	28.71	38.66	39.11
\mathcal{L}_t	(MeV)	22.44	24.83	21.15	25.12

III. NUCLEAR MATTER PROPERTIES

Energy of the nuclear matter is a function of $\rho = \sum_{\sigma\tau} \rho_{\tau\sigma}$, $\eta_s = \sum_{\sigma\tau} \sigma \rho_{\tau\sigma} / \rho$, $\eta_t = \sum_{\sigma\tau} \tau \rho_{\tau\sigma} / \rho$ and $\eta_{st} = \sum_{\sigma\tau} \sigma\tau \rho_{\tau\sigma} / \rho$ in the HF approximation, with $\rho_{\tau\sigma}$ ($\tau = p, n$ and $\sigma = \uparrow, \downarrow$) stands for densities depending on the spin and the isospin. Formulas to calculate the nuclear matter energy and its derivatives for given $\rho_{\tau\sigma}$ have been derived in Ref. [2].

The energy per nucleon $\mathcal{E} = E/A$ has its minimum \mathcal{E}_0 , at the saturation density ρ_0 (equivalently, k_{F0}). The incompressibility and the volume symmetry energy are defined by

$$\mathcal{K} = 9\rho^2 \left. \frac{\partial^2 \mathcal{E}}{\partial \rho^2} \right|_0, \quad a_t = \left. \frac{1}{2} \frac{\partial^2 \mathcal{E}}{\partial \eta_t^2} \right|_0. \quad (2)$$

Here $|_0$ indicates evaluation at the saturation point. The curvatures with respect to η_s and η_{st} are denoted by a_s and a_{st} . The k -mass M_0^* is defined by a derivative of the s.p. energy. Density-dependence of the symmetry energy is typically represented by

$$\mathcal{L}_t = \left. \frac{3}{2} \rho \frac{\partial^3 \mathcal{E}}{\partial \rho \partial \eta_t^2} \right|_0. \quad (3)$$

These quantities calculated from the new semi-realistic interactions are tabulated in Table II. For comparison, the values obtained by the D1S [7] and D1M [8] parameter-set of the Gogny interaction are also displayed. We also present the Landau-Migdal (LM) parameters in Table III, which are calculated by using the formulas given in Ref. [2]. See Ref. [2] also for definition of the LM parameters. It has been known that $g'_0 \approx 1$ [9], which is reproduced by the semi-realistic M3Y-type interactions primarily due to $v_{\text{OPEP}}^{(C)}$.

For the symmetric nuclear matter, M3Y-P4' and P5' give $\mathcal{E}(\rho)$ very close to each other, and also to those of M3Y-P4 and P5 [3]. $\mathcal{E}(\rho)$ in the neutron matter is shown in Fig. 1. As in M3Y-P4 and P5, the ρ -dependence of the SE channel in M3Y-P4' and P5' gives sizable repulsion at high ρ , by which $\mathcal{E}(\rho)$ is qualitatively similar to the result of Ref. [10], unlike the D1S case.

TABLE III. Landau-Migdal parameters at the saturation point.

	D1S	D1M	M3Y-P4'	M3Y-P5'
f_0	-0.369	-0.255	-0.327	-0.318
f_1	-0.909	-0.762	-1.042	-1.089
f_2	-0.558	-0.302	-0.431	-0.363
f_3	-0.157	-0.058	-0.208	-0.182
f'_0	0.743	0.701	0.499	0.458
f'_1	0.470	0.378	0.631	0.600
f'_2	0.342	0.633	0.245	0.245
f'_3	0.100	0.137	0.096	0.096
g_0	0.466	-0.013	0.228	0.216
g_1	-0.184	-0.380	0.263	0.255
g_2	0.245	0.483	0.162	0.168
g_3	0.091	0.114	0.078	0.080
g'_0	0.631	0.711	1.033	1.007
g'_1	0.610	0.652	0.180	0.146
g'_2	-0.038	-0.243	0.034	0.044
g'_3	-0.036	-0.064	-0.004	0.008

IV. APPLICATION TO FINITE NUCLEI

The HF and HFB calculations are implemented in finite nuclei by using the Gaussian expansion method [11–14] and adopting the Hamiltonian $H = H_N + V_C - H_{c.m.}$, where H_N , V_C and $H_{c.m.}$ represent the effective nuclear Hamiltonian, the Coulomb interaction and the center-of-mass Hamiltonian. The exchange term of V_C is treated exactly. Both the one- and the two-body terms of $H_{c.m.}$ are subtracted before iteration.

The binding energies and rms matter radii of several doubly magic nuclei are calculated in the spherical HF approximation. The results of the new semi-realistic interactions are compared with those of D1S and D1M, as well as with the experimental data, in Table IV. The new interactions reproduce the binding energies and the rms matter radii with similar accuracy to M3Y-P4 and P5. The deviation in the binding energies is $\lesssim 10$ MeV. Though slightly worse than D1S and D1M, we do not take this deviation seriously, until correlations due to the residual interaction are taken into account.

In M3Y-P4' and P5', some of the parameters in the SE channel are fitted to the even-odd mass differences $\Delta_{\text{mass}}^Z(N) = E(Z, N) - \frac{1}{2}[E(Z, N+1) + E(Z, N-1)]$ ($N = \text{odd}$) of the $66 \leq N \leq 80$ Sn isotopes, in the spherical HFB approximation with the $\ell \leq 7$ basis truncation. Contribution of $v_{ij}^{(DD)}$ to the pairing is fully taken into account. The equal filling

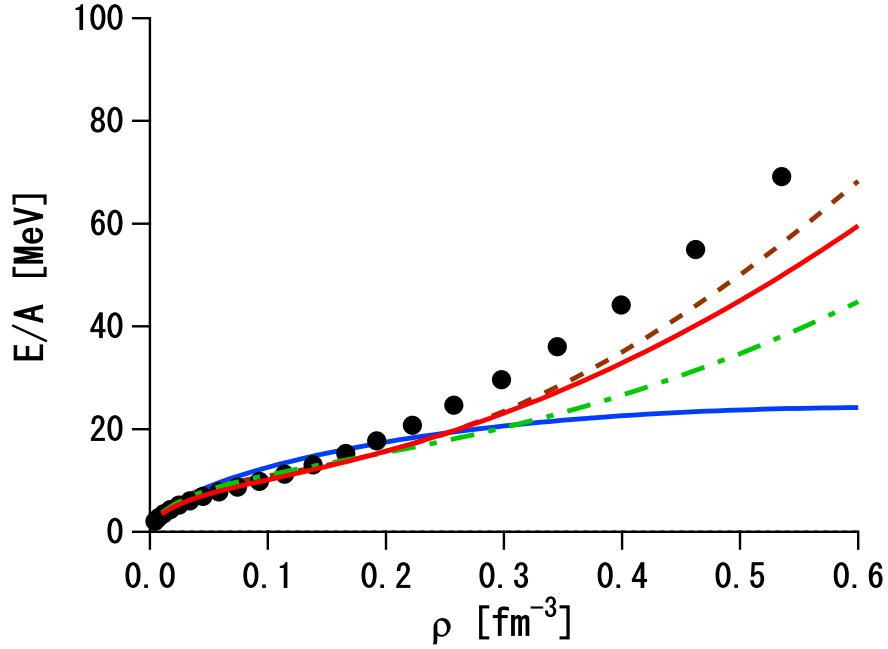


FIG. 1. Energy per nucleon $\mathcal{E} = E/A$ in the neutron matter. Blue solid, brown dotted, green dot-dashed and red solid lines represent the results with the D1S, D1M, M3Y-P4' and P5' interactions, respectively. Circles are the result of Ref. [10].

TABLE IV. Binding energies and rms matter radii of several doubly magic nuclei. Experimental data are taken from Refs. [15–18].

		Exp.	D1S	D1M	M3Y-P4'	M3Y-P5'
^{16}O	$-E$ (MeV)	127.6	129.5	128.2	127.8	124.1
	$\sqrt{\langle r^2 \rangle}$ (fm)	2.61	2.61	2.57	2.59	2.60
^{24}O	$-E$ (MeV)	168.5	168.6	167.3	166.6	166.4
	$\sqrt{\langle r^2 \rangle}$ (fm)	3.19	3.01	2.98	3.02	3.02
^{40}Ca	$-E$ (MeV)	342.1	344.6	342.2	338.7	331.7
	$\sqrt{\langle r^2 \rangle}$ (fm)	3.47	3.37	3.33	3.36	3.37
^{48}Ca	$-E$ (MeV)	416.0	416.8	414.6	412.0	411.5
	$\sqrt{\langle r^2 \rangle}$ (fm)	3.57	3.51	3.48	3.51	3.51
^{90}Zr	$-E$ (MeV)	783.9	785.9	782.1	776.9	775.7
	$\sqrt{\langle r^2 \rangle}$ (fm)	4.32	4.24	4.20	4.23	4.23
^{132}Sn	$-E$ (MeV)	1102.9	1104.1	1104.5	1100.8	1100.6
	$\sqrt{\langle r^2 \rangle}$ (fm)	—	4.77	4.72	4.77	4.76
^{208}Pb	$-E$ (MeV)	1636.4	1639.0	1638.9	1634.7	1635.7
	$\sqrt{\langle r^2 \rangle}$ (fm)	5.49	5.51	5.47	5.51	5.51

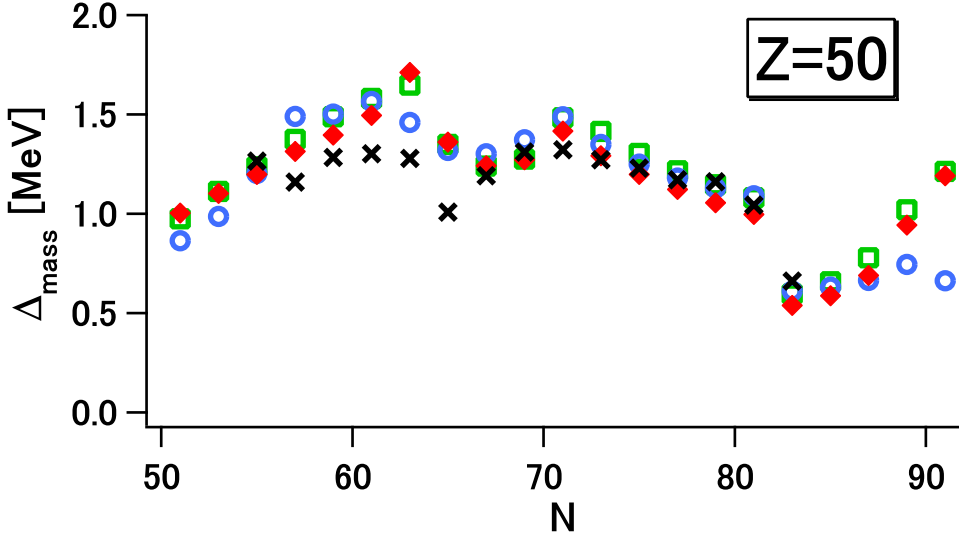


FIG. 2. Even-odd mass difference in the Sn isotopes, $\Delta_{\text{mass}}^{Z=50}(N)$. The results of D1S, M3Y-P4' and M3Y-P5' are shown by blue open circles, green open squares and red diamonds, respectively. Experimental values, presented by black crosses, are taken from Ref. [18].

approximation [19] is applied to the odd-mass nuclei. See arguments in Ref. [3] on influence of the ℓ truncation, the particle-number conservation and the non-spherical mean fields. $\Delta_{\text{mass}}^{Z=50}(N)$ calculated by M3Y-P4' and P5' are compared with the experimental data and with those obtained by D1S in Fig. 2. Though not shown, D1M gives $\Delta_{\text{mass}}^{Z=50}(N)$ quite close to that of D1S except at $N = 92$. The mass difference at $N \sim 64$ and 90 reflects interaction-dependence of the shell structure. In the M3Y-P4' and P5' interactions the $N = 64$ subshell effect is stronger than in D1S. At $N \sim 90$ the M3Y-type interactions yield larger mass difference than D1S, because $n1f_{7/2}$ and $n2p_{3/2}$ well mix due to the pairing.

We depict difference between the HF and the HFB energies, which represents the pair correlation, for the Ca nuclei in Fig. 3 and for the Ni isotopes in Fig. 4. These results are qualitatively similar to those shown in Ref. [3]. However, we dare to repeat several interesting points. The vanishing difference between the HF and HFB energies is normally connected to the shell closure. It is found that ^{52}Ca is nearly a doubly-magic nucleus with any of the interactions, as is consistent with the experiments [20]. With M3Y-P5', ^{68}Ni is almost doubly magic in harmony with experimental data [21], although ^{60}Ca is not. This suggests significant Z -dependence of the shell structure around $N = 40$, whose origin will be argued elsewhere. The hindrance of the pair excitation at ^{86}Ni suggests magic or submagic nature of $N = 58$ due to the gap between $n2s_{1/2}$ and $n1d_{3/2}$.

Prediction of the neutron drip line depends on effective interactions to a certain degree. Compared to the results with M3Y-P4 and P5 [3], more neutron-rich Ca and Ni nuclei are bound with M3Y-P4' and P5'. The heaviest bound Ca (Ni) nucleus has $N = 50$ (66) in both

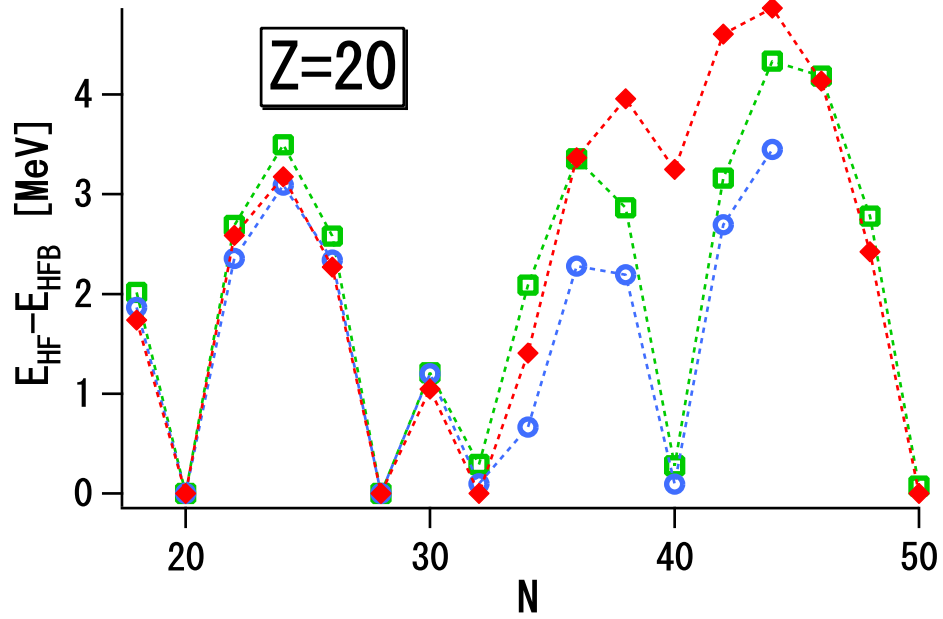


FIG. 3. Difference between the HF and HFB energies for the Ca isotopes ($N = \text{even}$), obtained from D1S, M3Y-P4' and P5'. See Fig. 2 for conventions. Dotted lines are drawn to guide eyes.

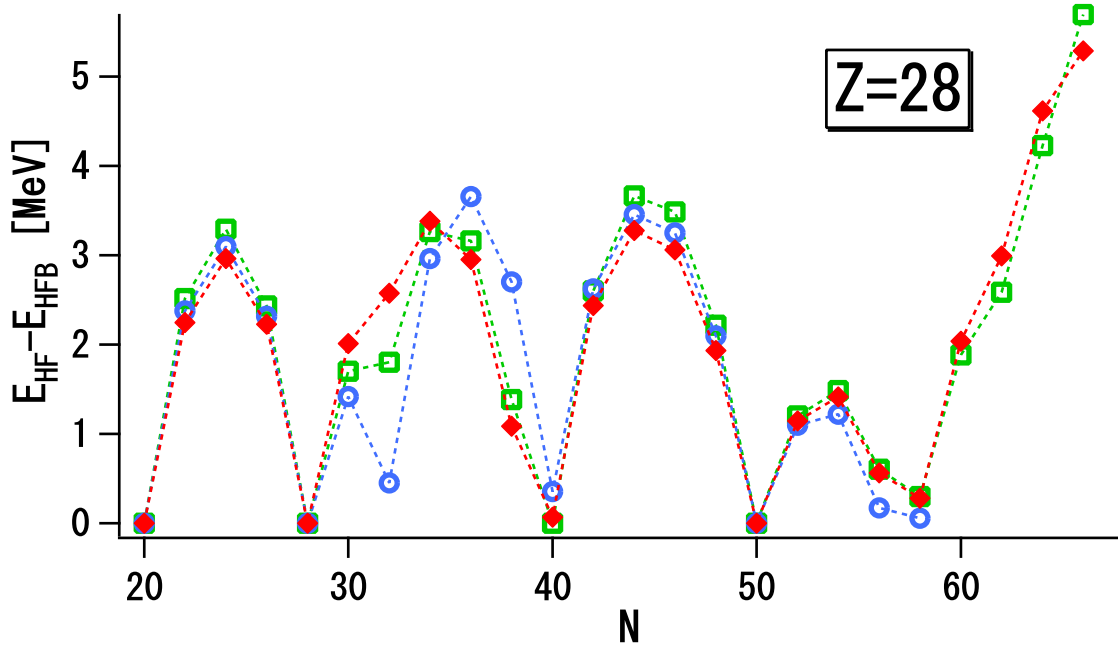


FIG. 4. Difference between the HF and HFB energies for the Ni isotopes ($N = \text{even}$). See Fig. 2 for conventions.

of the M3Y-P4' and P5' results.

V. SUMMARY

We have obtained new parameter-sets of the M3Y-type semi-realistic effective interaction to describe structure of nuclei, by taking into account the whole contribution of the interaction to the pairing in the HFB calculations. Two new parameter-sets have been presented; one keeping the tensor force of the M3Y-Paris interaction (M3Y-P5'), and the other discarding the tensor force (M3Y-P4'). The OPEP part in the central force is maintained. Basic characters of the interactions are examined in the infinite nuclear matter and in several doubly magic nuclei. The pairing properties are checked by the even-odd mass difference of the Sn isotopes in the HFB approximation. Pair energies and location of the neutron drip line are investigated for the Ca and Ni isotopes. The results do not change significantly from the previous ones, in which influence of the density-dependent contact force on the pairing was partly discarded.

ACKNOWLEDGMENTS

This work is financially supported as Grant-in-Aid for Scientific Research (C), No. 19540262, by Japan Society for the Promotion of Science. Numerical calculations are performed on HITAC SR11000 at Institute of Media and Information Technology, Chiba University, at Information Technology Center, University of Tokyo, and at Information Initiative Center, Hokkaido University.

-
- [1] G. Bertsch, J. Borysowicz, H. McManus and W.G. Love, Nucl. Phys. **A284**, 399 (1977).
 - [2] H. Nakada, Phys. Rev. C **68**, 014316 (2003).
 - [3] H. Nakada, Phys. Rev. C **78**, 054301 (2008).
 - [4] T. Otsuka, T. Suzuki, R. Fujimoto, H. Grawe and Y. Akaishi, Phys. Rev. Lett. **95**, 232502 (2005).
 - [5] T. Shizuma *et al.*, Phys. Rev. C **78**, 061303(R) (2008).
 - [6] N. Anantaraman, H. Toki and G.F. Bertsch, Nucl. Phys. **A398**, 269 (1983).
 - [7] J.F. Berger, M. Girod and D. Gogny, Comp. Phys. Comm. **63**, 365 (1991).
 - [8] S. Goriely, S. Hilaire, M. Girod and S. Pèru, Phys. Rev. Lett. **102**, 242501 (2009).
 - [9] C. Gaarde *et al.*, Nucl. Phys. **A369**, 258 (1981); T. Suzuki, Nucl. Phys. **A379**, 110 (1982); G. Bertsch, D. Cha and H. Toki, Phys. Rev. C **24**, 533 (1981); T. Suzuki and H. Sakai, Phys. Lett. **B455**, 25 (1999).
 - [10] B. Friedman and V.R. Pandharipande, Nucl. Phys. **A361**, 502 (1981).

- [11] H. Nakada and M. Sato, Nucl. Phys. **A699**, 511 (2002); *ibid.* **A714**, 696 (2003).
- [12] H. Nakada, Nucl. Phys. **A764**, 117 (2006); *ibid.* **A801**, 169 (2008).
- [13] H. Nakada, Nucl. Phys. **A808**, 47 (2008).
- [14] H. Nakada, K. Mizuyama, M. Yamagami and M. Matsuo, Nucl. Phys. **A828**, 283 (2009).
- [15] D.T. Khoa, H.S. Than and M. Grasso, Nucl. Phys. **A722**, 92c (2003).
- [16] A. Ozawa *et al.*, Nucl. Phys. **A691** (2001) 599.
- [17] G.D. Alkhasov, S.L. Belostotsky and A.A. Vorobyov, Phys. Rep. **42**, 89 (1978).
- [18] G. Audi and A.H. Wapstra, Nucl. Phys. **A595**, 409 (1995).
- [19] S. Perez-Martin and L.M. Robledo, Phys. Rev. C **78**, 014304 (2008).
- [20] J.I. Prisciandaro *et al.*, Phys. Lett. **B510**, 17 (2001).
- [21] R. Broda *et al.*, Phys. Rev. Lett. **74**, 868 (1995).